Asia-Pacific Journal of Science and Technology: Volume: 28. Issue: 06. Article ID.: APST-28-06-09. Research Article

APST

Asia-Pacific Journal of Science and Technology

https://www.tci-thaijo.org/index.php/APST/index

Published by the Research and Graduate Studies Division,
Khon Kaen University, Thailand

Modelling and analysis of new organic thin film temperature sensor

Arun P.S. Rathod[1] and Abhilasha Mishra[2,*]

[1]Department of Electronics and Communication, Graphic Era Hill University, Dehradun, India
[2]Department of Chemistry, Graphic Era (Deemed to be University), Dehradun, India
[*]Corresponding author: abhi1680@geu.ac.in

Received 21 July 2022
Revised 31 October 2022
Accepted 16 November 2022

Abstract

Integration of sensor modules in contemporary smart devices is imperative for initiating automation in the devices. Among such sensors temperature sensors based on conventional inorganic semiconductors are most common. Temperature sensors are generally used in various electronic devices like smart watches, digital thermometers, digital weather stations etc. Integration of inorganic temperature sensor modules in such organic smart devices adds to circuit complexity, inconsistency, increment in fabrication cost and size of the device. In this research article a new flexible organic thin film temperature sensor is proposed that is inspired from the operational functionality of organic thin film transistors. The proposed organic thin film temperature sensor (OTS) is structurally and behaviourally similar to an organic thin film transistor (OTFT). A comparative analysis of OTS with single gate and dual gate OTFT structures using modelling and simulation is performed to validate its functionality and determine its operational efficiency across different performance parameters. The OTS is found to generate 167% and 17% more drain current then single gate and double gate (DG) OTFTs respectively with same material composition, and voltage regime. Also, OTS has 31% higher temperature sensitivity compared to double gate OTFTs. It will eliminate the need of additional circuit components required to make contemporary inorganic temperature sensors functional with smart organic electronic devices. Hence the proposed OTS being dimensionally and functionally equivalent to a single OTFT could replace the conventional inorganic semiconductor-based temperature sensors to achieve fabrication compatibility and size optimization in modern organic electronic devices.

Keywords: Organic, OTFT, OTS, Smart devices, Temperature sensor, Wearable electronics

1. Introduction

Among the different natural phenomenon, measurement of 'heat' is most common. Heat is measured in terms of temperature that is defined as the average of kinetic energy possessed by atoms/molecules in any system. It is an expression of energy in thermal form, that is omnipresent in all type of matter and act as the source of heat generation, and energy flow from hotter to colder body. Temperature sensors are used to detect the degree of heat energy present within a matter or in its surrounding. Temperature sensors are widely used in manufacturing industries, health care facilities, scientific research, automation, smart wears etc. Consequently, the volume of thermal or temperature sensors make up the largest portion of contemporary sensing device industry [1]. Different physical quantities (like pressure, humidity, gas concentration etc.) are also dependent on temperature, therefore devices used for measuring such quantities are also required to integrate temperature sensors to compensate for temperature related measurement deviations [2]. There are numerous techniques employed for measuring temperature that exploit physical properties of matter like thermal expansion [2] thermoelectricity [3], fluorescence [4], etc. Generally, temperature sensing systems are divided in to three broad categories viz. non-invasive, semi-invasive and invasive [3,5,6]. These categories have their distinct advantages and restrictions. An invasive type of sensor is required to be inserted inside the object to measure its temperature. Such devices are largely used in the healthcare or pharmaceutical industry [8], beverage and food industry, scientific laboratories etc. These include oral thermometers, rectal thermometers etc. They are accurate but invades personal space of

the user and may cause hygiene related issues. Semi-invasive type sensor can measure the temperature by making the contact with the surface of an object. Most common example of such sensor include skin temperature sensor used in smart watches. The non-invasive type of temperature sensor includes infrared thermometers, optical pyrometers, broadband radiation thermometers etc. Such sensors are preferred for assessing temperature of moving objects that are small in size and not accessible easily and for processes that are dynamic in nature and require fast response; and for temperatures <1000°C (1832°F).

In the field of smart fabrics and wearable electronics non-invasive temperature sensors are used to identify different temperatures ranges to attain certain degree of automation [8]. In contemporary smart wear devices under internet of things (IOT) framework, organic semiconductor based sensors are used due to their low price and easy integration [9-13]. Integrating inorganic sensors with otherwise organic smart wear devices may result in higher cost of production as well as inefficiency in circuit integration due to mismatch in size and physical properties of organic and inorganic transistors. It may also increase the overall size of the smart devices as additional circuitry is required to integrate the inorganic temperature sensors with the organic smart devices. Therefore, there is a requirement of a temperature sensor based on organic semiconductor that could be homogeneously integrated with the organic smart devices without increasing the device size and fabrication cost. To address this need, a new organic thin film temperature sensor (OTS) is proposed in this research work with single drain electrode and double source electrode structure through modelling and simulation. This sensor is similar in size and behaviour to a double gate organic thin film transistor and could be integrated in the circuit of the smart device without any additional supporting circuit components. The research article is subdivided into four sections. Section 1 is dedicated to introduction to the problem statement, whereas Section 2 elucidates design and analysis of organic thin film temperature sensor. Results are discussed in Section 3 and conclusion is presented in the Section 4.

2. Materials and methods

The design of OTS sensor is based on the concept of migration of the charge carriers under the influence of an electric field [13]. The sensor experiences alteration in output drains current level under different temperature regimes. The objective of this research is to develop an organic thin film transistor that could also perform as a temperature sensor. Therefore, the performance of proposed OTS is compared with the bottom gate bottom contact (BGBC) organic thin film transistor (OTFT), double gate (DG) OTFT, which are widely used single gate and dual gate OTFT structures respectively using modelling and simulation. The performance will be analysed in terms of the mobility of the charge carriers, output drain current and ability to sense the temperature over wider range. Structural configuration of BGBC OTFT, DG OTFT and OTS are displayed in Figure 1 (A), (B) and (C) respectively. BGBC OTFT is comprised of single gate electrode with one source and one drain electrode in addition to an OSC layer and a dielectric layer. Whereas DG OTFT has two gate and dielectric layers viz. top and bottom layers. The structure of OTS is comprised of two gate electrodes (top and bottom), a couple of dielectric thin films (top and bottom), single organic semiconductor layer (OSC), double source electrodes (top and bottom) and single drain electrode.

To evaluate the effect of temperature on (OTS), the structure of temperature sensor is investigated using organic module standard incorporated in Atlas 2-D TCAD simulator from SILVACO. For result prediction under various boundary limitations, the Poole-Frenkel model for mobility is employed [14]. The conduction channel formation inside BGBC OTFT, DG OTFT and OTS on application of suitable biasing voltage is shown in Figure 2 (A), (B) and (C) respectively. It is evident from Figure 2 (C) that OTS generates two distinct conduction channels, and it is a functional OTFT like BGBC OTFT and DG OTFT. For simulation purpose, an efficient current model called Poole-Frenkel model was utilized by summing up the currents generated due to injection or ejection of charge carriers at the material interfaces, determined through thermionic emission. In this model the transport of charge carriers inside dielectric materials is determined by the diffusion or the drifting of the holes or electrons in a semiconductor material with greater energy band gap. Apart from the applied voltage (electric field), different parameters were varied namely the trap density associated with acceptors and donors; the level of energy associated with the traps at zero-field energy within energy band gap, the internal Schottky effect modifies this energy level; dielectric layer thickness; the dielectric layer permittivity related to different oxide materials; the potential barriers associated with charge carriers at the interfaces of various electrode materials; at constant temperature.

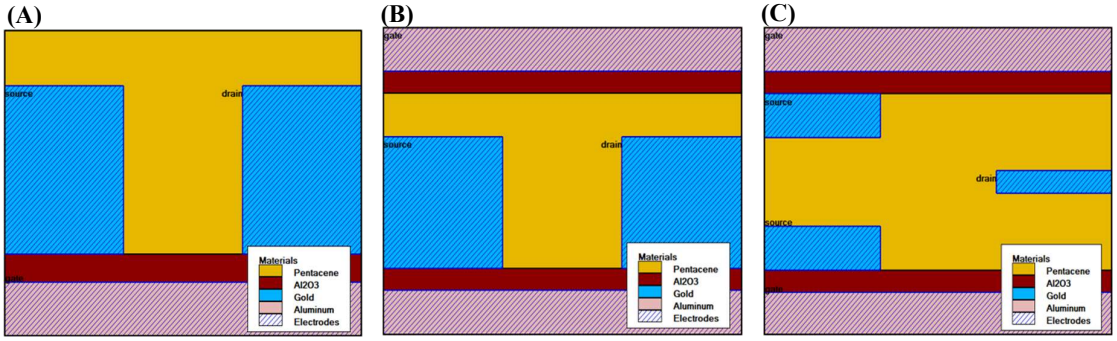

Figure 1 2-D simulated structural representation of (A) BGBC OTFT. (B) DG OTFT. (C) OTS.

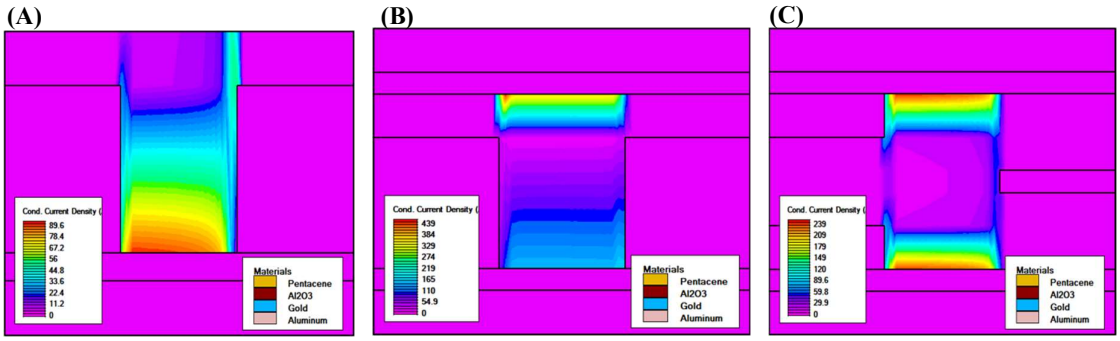

Figure 2 Conduction channel formation inside simulated (A) BGBC OTFT. (B) DG OTFT (C) OTS.

The Poole-Frenkel model facilitates visualization of conduction which is result of thermal excitation due to enhancement in field of trapped charges. Materials and dimensions used in modelling and analysis of OTS are recorded in Table 1. The OTS incorporates novel single drain double source (SDDS) architecture for enhanced temperature sensitivity. When a suitable external voltage is applied between gate and source electrodes (both top and bottom respectively), the charge carries starts accumulating in the conduction channel region near the interface of dielectric layer and OSC layer [15-17]. Consequently, if required voltage biasing is provided between source and drain electrode, the accumulated charge carries start moving from source in the direction of drain electrode resulting in the formation of conducting channel [18]. Since the OTS has two gate electrodes, two distinct channels are formed as depicted in Figure. 2 (C). The dual source structure makes the OTS very sensitive as alterations in the drain current may occur with minor changes in the temperature. OTS makes temperature assessment by measuring the fluctuations in drain current levels corresponding to different temperature regimes [7].

At the material level, in pentacene (OSC material used in the current research) rise in temperature results in energizing of charge carriers. These energized charge carriers fill the trap locations inside pentacene layer. On the other hand, in silicon the energized charge carriers start moving randomly in all directions. As a result, overall current inside the silicon layer deteriorates. Also, organic semiconductor materials like Pentacene, contain substantial trap energy states in their energy band [17,19,20] whereas inorganic material like silicon does not have such traps, as shown in Figure 3. Consequently, temperature sensor comprised of inorganic semiconductor materials like silicon becomes unreliable after a threshold temperature is breached. The random movement of charge carriers in such materials give rise to random fluctuations in output drain current, due to this precise measurement of the temperature could not be achieved. Whereas in organic semiconductors like pentacene the activation energy (α) of charge carriers decreases with increase in temperature and with increment in negative bias gate to source voltage (V_{GS}), new charges are generated. These newly spawn charge carriers fill the additional localized trap states and flow of charge becomes smooth. Consequently, the energy required for charge carriers to reach the HOMO energy level is reduced [1,21]. As a result of this phenomenon the output drain current I_{DS}, in organic thin film transistors increases with rise in temperature. Hence, the organic thin film temperature sensor is better and reliable alternative for silicon based contemporary temperature sensors for measuring temperature variations.

Table 1 Physical parameters and material composition used in modelling of BGBC OTFT, DG OTFT and OTS.

Thin Films	BGBC OTFT	DG OTFT	OTS
OSC Layer	Pentacene, 80nm	Pentacene, 80nm	Pentacene, 80nm
Source Electrode (top & bottom)	Gold, 60nm	Gold, 60nm	Gold, (20nm + 20nm)
Drain Electrode	Gold, 60nm	Gold, 60nm	Gold, 20nm
Gate Electrode (top & bottom)	Aluminium, 20nm	Aluminium, (20nm + 20nm)	Aluminium, (20nm + 20nm)
Dielectric Layer (top & bottom)	Al_2O_3,10nm	Al_2O_3 (10nm + 10nm)	Al_2O_3 (10nm + 10nm)

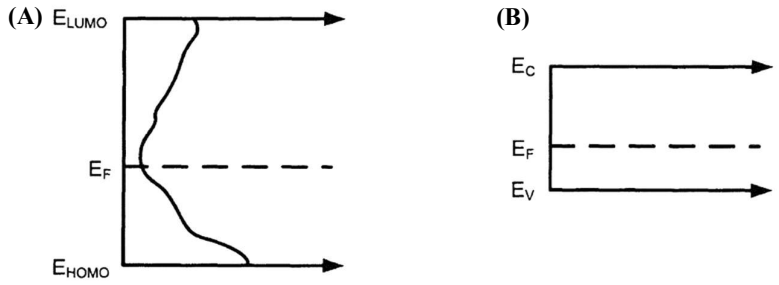

Figure 3 Trap density between energy bands in (A) organic and (B) inorganic semiconductor respectively.

The organic semiconductor layer comprised of Pentacene could be fabricated through solution processing or thermal evaporation. Similarly, dielectric layer of aluminium oxide could be deposited through solution processing or thermal evaporation. For deposition of source and drain electrodes shadow masking, lithography, lift off or transfer printing could be used. The aluminium gate electrode could be deposited through vacuum thermal evaporation [18,23,24]. Since the structure of OTS have source and drain electrodes in three different positions, therefore OSC will be deposited in three part to accommodate the thermal deposition of source and drain electrode unlike BGBC and DG OTFT where OSC layer is deposited in a single attempt.

3. Results and discussion

Organic thin film temperature sensor structure used in the analysis is comprised of five different material layers and three embedded electrodes. Initially an aluminium layer is deposited over a flexible substrate through vacuum thermal deposition. This layer will serve as the bottom gate electrode of the organic thin film transistor sensor. Over the bottom gate electrode layer a thin film of aluminium oxide is deposited by employing thermal evaporation or RF magnetron sputtering, to eliminate the migration of charge between organic semiconductor layer (pentacene) deposited over it and gate electrode layer. Bottom source electrode is deposited through transfer printing over dielectric layer. A 40nm thick pentacene layer is deposited over the dielectric layer through thermal deposition enveloping the bottom source electrode.

Over this layer drain electrode of gold is deposited through transfer printing. Again, a pentacene layer is deposited with 20nm thickness, engulfing the drain electrode. Top source electrode of gold is deposited over it through transfer printing and final pentacene layer of 20nm is deposited completing the embedding of the source and drain electrodes inside OSC layer. Over the OSC layer another thin film of aluminium oxide is deposited through RF magnetron sputtering. Finally, the top gate electrode layer of aluminium is deposited through physical vapour deposition technique. For sensing temperature by measuring variations in drain current, it is imperative that OTS should be functionally similar to an OTFT. To ascertain the functional correctness and operational accuracy of the OTS, analysis is carried out at 273 K and performance of OTS across different performance parameters is compared with performance of BGBC and DG OTFT for same parameters. The results are recorded in Table 2. It has been found in the analysis that the proposed SDDS structure of OTS is functionally similar to BGBC and DG OTFT as the movement of charge carriers takes place under the effect on an external electric field. The drain current generation of OTS i.e., 7.98 μA is highest among the three devices taken for analysis as shown in Table 2. It means that the OTS could sense wider range of temperature as compared to BGBC and DG OTFT. Also, the ratio of 'ON' current to 'OFF' current is highest for the OTS (1.92×10^6) signifying the lower value of thermally generated subthreshold leakage current. The lower leakage current makes the OTS more thermally stable over greater temperature variations as compared to BGBC and DG OTFT. Further the mobility of charge carriers in the linear region is greatest inside OTS (7.14 $cm^2/V.\ s$).

This makes OTS more sensitive towards temperature fluctuation as compared to DG or BGBC OTFT where charge carriers have lower mobility. In addition to higher carrier mobility, lower threshold voltage also enhances

the temperature sensitivity of the OTS as it could become operational at lower voltage then the other two devices viz. BGBC OTFT and DG OTFT. Result magnitudes recorded in the Table 2 have an error margin of ±0.68. The organic thin film temperature sensor owing to its novel structure generates two conduction channels in the organic semiconductor layer as shown in Figure 2 (C). Since the accumulation of charge takes place at the interface of OSC layer and dielectric layer, large number of charge carriers is accumulated near top and bottom dielectric and due to bi-positional source electrodes higher drain current with enhanced mobility is obtained. Whereas in BGBC OTFT accumulation of charge carriers takes place in the limited region between source and drain electrode, thus lower number of charge carries could accumulate and hence the drain current produced by BGBC OTFT is lowest amongst three devices taken for analysis with same OSC layer and voltage regime. In case of DG OTFT two channels are formed but with different intensity as shown in Figure 2 (B). The bottom channel of DG OTFT is weaker due to the lower charge accumulation like BGBC OTFT, whereas the top channel is strong as greater number of charge carriers could accumulate in the top channel region.

Table 2 Performance of OTS across different parameters achieved after the simulation analysis.

Performance Parameters	BGBC OTFT	DG OTFT	OTS
Gate to Source Voltage, V_{GS} (V)	0 to -3	0 to -3	0 to -3
Drain to Source Voltage, V_{DS} (V)	-1.5	-1.5	-1.5
Drain current, Ids (μA)	2.98	6.8	7.98
I_{ON}/I_{OFF} ratio	978.44	3.9×10^{5}	1.92×10^{6}
Transconductance, gm (μS)	2.57	4.06×10^{-6}	5×10^{-6}
Mobility linear, μ_{lin} ($cm^2/V.\ s$)	3.67	5.81	7.14
Threshold voltage, Vth (V)	-1.84	-1.40	-1.30
Sub-Threshold Slope, SS (V/dec)	0.59	0.09	0.08

Therefore, greater the charge accumulation in the conduction channel region of any OTFT, higher the drain current will be produced and superior will be the charge carrier mobility. Hence, the novel structure of OTS is justified, as it enables maximum charge accumulation in the conduction channel region. After determining the behavioural output of OTS and validating its performance, the devices are further analysed using SILVACO Atlas TCAD simulator to determine the nature of variations in drain current due to temperature fluctuations under same voltage regime at five different temperature profiles viz. 250K, 273K, 300K, 325K, 350K. The output drains current thus obtained is verified mathematically using drain current equations for OTFTs via. Equation (1) and Equation (2).

$$I_{Dlin} = \frac{W}{L} \times \mu_n C_{ox} \left[V_{GS} - \frac{V_{DS}}{2} - V_T\right] \times V_{DS} \quad (1)$$

$$I_{Dsat} = \frac{1}{2} \times \frac{W}{L} \times \mu_n C_{ox} [V_{GS} - V_T]^2 \quad (2)$$

Here, W and L represents width and length of the conduction channel respectively, μ_n is mobility of the charge carriers whereas C_{ox} is lumped oxide capacitance. V_T represents threshold voltage, V_{DS} and V_{GS} are drain to source voltage and gate to source voltage respectively. I_{Dsat} represents drain current in saturation regime whereas I_{Dlin} represents drain current in linear regime.

Since the applied voltages were same for all the devices with no change in size or material composition, the alteration seen drain current of the devices was the direct result of temperature variation as shown in Figure. 4. All three devices have shown variations in drain current with changing temperature. The temperature dependent variations in the drain current of BGBC OTFT are minimum as displayed in Figure 4 (A), making it unsuitable for temperature sensing. On the other hand, the DG OTFT device show greater variations in output drain current with change in temperature as depicted in Figure 4 (B). The variation in drain current of DG OTFT is quite distinct and drain current levels are also higher as compared to BGBC OTFT. The drain current plots of organic thin film temperature sensor with respect to different temperature profiles are displayed in Figure 4 (C). It is evident from the Figure 4 (D) that for any given temperature profile highest magnitude of drain current is produced by OTS. It is an important property for temperature sensor as higher the magnitude of drain current, more profound will be the variations in it with respect to change in temperature. It is visible in Figure 4 that with increment in drain voltage the drain current magnitudes of OTS are increasing at greater rate than BGBC or DG OTFT for every temperature profile. Also, in OTS and DG OTFT the drain current is still in linear region whereas in BGBC OTFT it has almost achieved saturation and show no change for any temperature variation after drain to source voltage (V_{DS}) becomes -3 V.

Another analysis is done to measure the temperature sensitivity of the devices by measuring the deviation in drain current magnitudes produced at lowest and highest temperature by the three devices at constant gate to source voltage (V_{GS}=-3V). The results of this analysis are displayed in Figure 5. The highest drain current is obtained when the temperature was set at 350K, whereas lowest drain current is obtained when temperature was 250K. The rise in temperature provides activation energy to the charge carriers, as a result more and more charge carriers acquire sufficient activation energy to jump from highest unoccupied molecular orbital (HOMO) to lowest unoccupied molecular orbital (LUMO). Due to this surge in number of charge carriers in LUMO (responsible for conduction current) the overall drain current magnitude in the OTS rises substantially. On the contrary, when the temperature declines the number of charge carriers in the LUMO diminishes. This is because only those charge carriers now gain sufficient activation energy to jump from HOMO to LUMO that are under the influence of electric field generated in OTS through voltage supply and contribute to the formation of conduction channel.

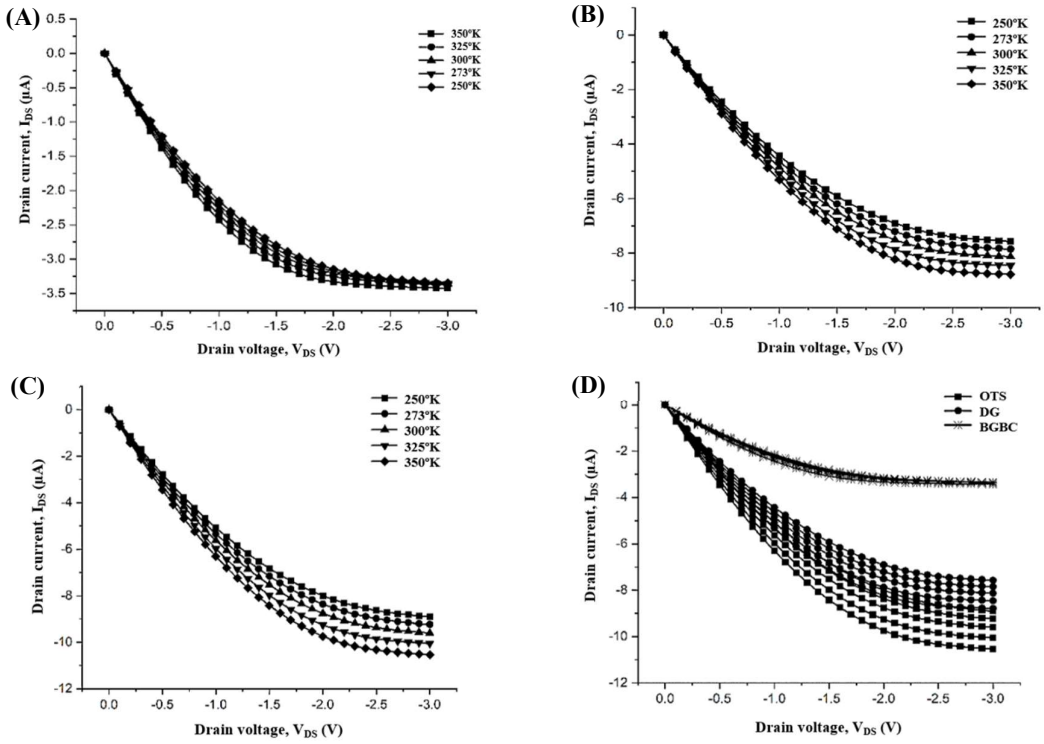

Figure 4 Temperature dependent variations at constant gate to source voltage (V_{GS} = -3V) in output drain current of simulated (A) BGBC OTFT, (B) DG OTFT, (C) OTS, (D) Combined.

It is apparent from Figure 5 (B) that with rise in thermal profile i.e., temperature, there is a substantial change in the output drain current of OTS and DG OTFT whereas in BGBC OTFT only a minimal variation is observed. This shows that for any given temperature the change in drain current of the OTS is highest. Data provided in Figure 5 (A) also support this claim where deviation between drain current at lowest temperature (250 K) and drain current at highest temperature (350 K) of all three devices are displayed. The deviation recorded in drain current of BGBC OTFT is 0.07 μA as highest and lowest drain currents recorded for BGBC OTFT are 3.42 μA and 3.35 μA. whereas in case of DG OTFT the drain current deviation is found to be 1.21 μA, which is significantly better than BGBC OTFT. Highest and lowest drain currents recorded for DG OTFT are 8.79 μA and 7.58 μA respectively. Greatest deviation of 1.59 μA in drain current is produced by OTS, which is approximately 31% higher than the deviation recorded for DG OTFT. The highest and lowest drain current of OTS are found to be 10.5 μA and 8.91 μA respectively.

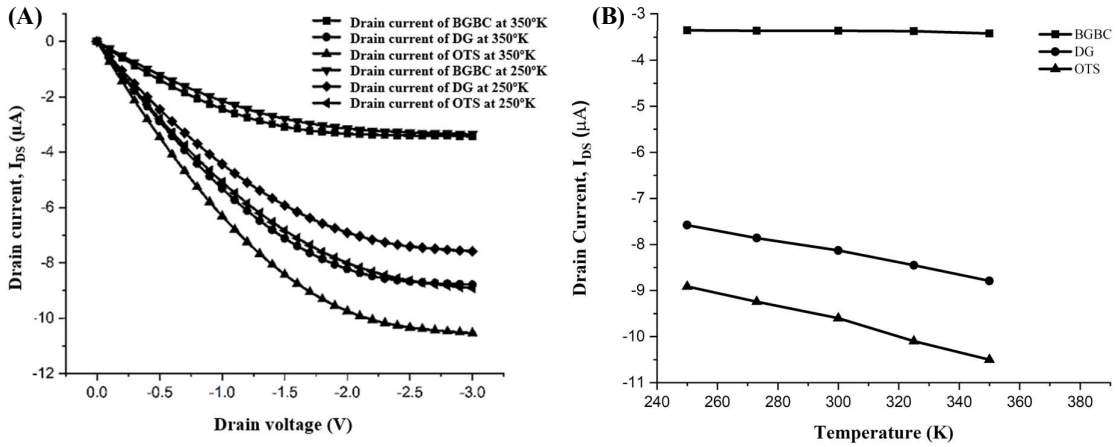

Figure 5 (A) Contrast in drain currents of simulated BGBC, DG and OTS devices for highest (350 K) and lowest (250 K) magnitude of temperature at constant V_{GS} = -3V, (B) Rise in drain current of simulated OTS with rise in temperature at constant V_{GS} = -3V and V_{DS} = -3V.

Hence, the OTS is most suited among the single gate and double gate OTFT structures for the role of temperature sensor. It has greater carrier mobility of 7.14 cm^2/V. s and generates higher drain current of magnitude 7.98 μA when V_{DS} is -1.5 V and V_{GS} is -3 V at 273 K as recorded in Table 2. Also, ratio of 'ON' current to 'OFF' current is highest for the OTS (1.92 x 10^6) signifying the lower value of thermally generated subthreshold leakage current. All these parameters conclusively prove that the proposed OTS is an efficient temperature sensor and could perform the dual role of an OTFT as well as an organic temperature sensor in an electronic circuit.

4. Conclusion

OTS measures the changes in temperature by monitoring the variations in the output drain current (I_{DS}). It has been established through modelling and simulation that in organic semiconductors like Pentacene, conductivity increases with increment in temperature and vice versa. After analysing proposed OTS with BGBC and DG OTFT at different temperatures, the OTS achieved the greatest deviation in I_{DS} (1.59 μA), highest charge mobility (7.14 cm^2/V. s) and maximum magnitude ranging between 8.91 μA and 10.5 μA. The analysis concludes that the proposed OTS is a viable and economical option to contemporary OTFT based organic temperature sensor technologies.

5. References

[1] Polena J, Afzal D, Ngai JHL, Li Y. Temperature sensors based on organic field-effect transistors. Chemosensors. 2022;10(1):12.
[2] Mansoor M, Haneef I, Akhtar S, De Luca A, Udrea F. Silicon diode temperature sensors-a review of applications. Sens Actuator A Phys. 2015;232:63-74.
[3] Childs PRN, Greenwood JR, Long CA. Review of temperature measurement. Rev Sci Instrum. 2000;71(8):2959-2978.
[4] Michalski L, Eckersdorf K, Kucharski JM. Temperature measurement. 2nd ed. Hoboken, New Jersey: Wiley; 2001.
[5] McGee. TD. Principles and methods of temperature measurement. 1st ed. New Jersey: Wiley; 1988.
[6] Altet J, Claeys W, Dilhaire S, Rubio A. Dynamic surface temperature measurements in ICs. Proc IEEE. 2006;94(8):1519-1532.
[7] Blackburn DL. Temperature measurements of semiconductor devices - a review. Annu IEEE Semicond Therm Meas Manag Symp. 2004;20:70-80.
[8] Yusof NS, Mohamed MFP, Ghazali NA, Khan MFAJ, Shaari S, Mohtar MN. Evolution of solution-based organic thin-film transistor for healthcare monitoring-from device to circuit integration: a review. Alexandria Eng J. 2022;61(12):11405-11431.
[9] Elkington D, Cooling N, Belcher W, Dastoor P, Zhou X. Organic thin-film transistor (OTFT)-based sensors. Electronics. 2014;3(2):234-524.
[10] Inal S, Malliaras GG, Rivnay J. Benchmarking organic mixed conductors for transistors. Nat Commun. 2017;8(1):1767.

[11] Lee MY, Lee HR, Park CH, Han SG, Oh JH. Organic transistor-based chemical sensors for wearable bioelectronics. Acc Chem Res. 2018;51(11):2829-2838.
[12] Wang N, Yang A, Fu Y, Li Y, Yan F. Functionalized organic thin film transistors for biosensing. Acc Chem Res. 2019;52(2):277-287.
[13] Fang X, Zong B, Mao S. Metal-organic framework-based sensors for environmental contaminant sensing. Nano-Micro Lett. 2018;10(4):64.
[14] SILVACO International. Silvaco User's Manual [Internet]. 2004 [cited 2022 Jun 12]. Available from: https://www.eng.buffalo.edu/~wie/silvaco/atlas_user_manual.pdf.
[15] Horowitz G. Organic field-effect transistors. Adv Mater. 1998;10(5):365-377.
[16] Kaushik BK, Kumar B, Prajapati S, Mittal P. Organic thin-film transistor applications. 1st ed. Florida: CRC Press; 2016.
[17] Kumar B, Kaushik BK, Negi YS. Organic thin film transistors: structures, models, materials, fabrication, and applications: a review. Polym Rev. 2014;54(1):33-111.
[18] Kalb WL, Mathis T, Haas S, Stassen AF, Batlogg B. Organic small molecule field-effect transistors with Cytop™ gate dielectric: eliminating gate bias stress effects. Appl Phys Lett. 2007;90(9):092104.
[19] Natali D, Caironi M. Charge injection in solution-processed organic field-effect transistors: physics, models and characterization methods. Adv Mater. 2012;24(11):1357-1387.
[20] Guo X, Xu Y, Ogier S, Ng TN, Caironi M, Perinot A, et al. Current status and opportunities of organic thin-film transistor technologies. IEEE Trans Electron Devices. 2017;64(5):1906-1921.
[21] Shim CH, Maruoka F, Hattori R. Structural analysis on organic thin-film transistor with device simulation. IEEE Trans Electron Devices. 2010;57(1):195-200.
[22] Shao M, He Y, Hong K, Rouleau CM, Geohegan DB, Xiao K. A water-soluble polythiophene for organic field-effect transistors. Polym Chem. 2013;4(20):5270.
[23] Wang BB, Zhu K, Feng J, Wu JY, Shao RW, Zheng K, et al. Low-pressure thermal chemical vapour deposition of molybdenum oxide nanorods. J Alloys Compd. 2016;661:66-71.